PERGAMON

International Journal of Solids and Structures 40 (2003) 715–727

INTERNATIONAL JOURNAL OF SOLIDS and STRUCTURES

www.elsevier.com/locate/ijsolstr

A shape control model for piezo-elastic structures based on divergence free electric displacement

M. Kekana *, P. Tabakov, M. Walker

Centre for Advanced Materials, Design and Manufacturing Research, Department of Mechanical Engineering, Durban Institute of Technology, P.O. Box 953, Durban 4000, South Africa

Received 28 November 2001; received in revised form 13 September 2002

Abstract

A model simulating the effects of the control potential on the static configuration of a piezo-elastic structure is presented. This model is centred on the electric displacement field, which is shown to be divergence free. Thus, the surface charge effect no control over the configuration of a piezo-elastic structure, save for the control potential derived through passive or active control. Results show that at zero gain the proposed model resembles a structure free from piezoelectric control. Thus, no fictituous stiffness is introduced as is the case with models presented in the literature.

Keywords: Piezo-elastic; Displacement; Structures

1. Introduction

Due to their adaptable properties, piezoelectric structural materials can function as distributed sensors and actuators for monitoring and controlling the response of a structure. In sensor applications, the strains on the piezoelectric material can be determined by measuring the induced electric potential. In actuator applications, distributed forces can be effected by subjecting the piezoelectric material to an appropriate control potential. By integrating piezoelectric elements into advanced composite materials, the potential for forming a high-strength, high-stiffness, lightweight structure capable of self-monitoring and adapting to changing operating conditions can be explored.

Models simulating the control of various structural elements have been developed and studied for this purpose. Two approaches in control using piezoelectric sensors have been adopted. The first assumes the signal from the sensor to be the electric current, viz. closed circuit mode (Hwang and Park, 1993; Miller et al., 1995; Chandrashekhara and Donthireddy, 1997; Yin and Shen, 1997). The other approach assumes the signal from the sensor to be the potential, viz. open circuit mode (Wang et al., 1997; Detwiler et al., 1995; Tzou and Tseng, 1990, 1991).

* Corresponding author. Fax: +27-31-204-2139.
E-mail address: kekanam@dit.ac.za (M. Kekana).

0020-7683/02/$ - see front matter
PII: S0020-7683(02)00611-X

The control model developed by assuming a closed circuit mode has been studied extensively by Miller et al. (1995). Results of the study show that applying suitable potentials on the piezoelectric elements via an amplifier can effect control of a structure. At zero gain, the structure is free from any piezoelectric control. Thus, the control model resembles the passive structure at this state.

Research conducted on the active control model of the open circuit mode has also shown that control can be effected through the piezoelectric elements (see Wang et al., 1997). However, these studies have not considered the bearing of the active control model at zero gain. Recent work, based on the current formulation of the open circuit mode control model, has provided a basis for developing a control model which resembles a passive structure at zero gain (Kekana and Walker, 2001; Kekana, 2001, 2002). The study initially performs a stability analysis of the control model (Kekana and Walker, 2001; Kekana, 2001). The criteria that emerge ensure that the control model depicts a stable response. However, results show that piezoelectric effects persist at zero gain (Kekana, 2002), contrary to the requirements stipulated in Miller et al. (1995).

This study proposes a control model of the open circuit mode which resembles the passive structure at zero gain. The model results from showing that the electric displacement is divergence free, thus indicating the non-controlling effect of the applied electric charge. On the contrary, the formulation of the control model found in the literature assumes the charge to be a function of the potential from the sensor layer, in active control. With the aid of an example, the current and proposed control models are compared numerically.

2. Energy formulation

Consider a composite structure to which are attached/embedded a pair of co-located piezoelectric elements for the purpose of sensing and actuating the shape of the host (see Fig. 1).

The shape control model based on the work density function which comprises piezoelectric, dielectric and elastic energy (Cady, 1946) and the external work is given by

$$W = \frac{1}{2}\int_{\Omega}\left(-\boldsymbol{\varepsilon}^{\mathrm{T}}\mathbf{C}\boldsymbol{\varepsilon} + 2\boldsymbol{\varepsilon}^{\mathrm{T}}\mathbf{e}\mathbf{E} + \mathbf{E}^{\mathrm{T}}\mathbf{g}\mathbf{E}\right)\mathrm{d}\Omega + \sum \mathbf{u}_i\mathbf{f}_i \tag{1}$$

where W is the work density function, $\boldsymbol{\varepsilon}$ is the strain vector, $\mathbf{C}$ is the elastic constants matrix, $\mathbf{e}$ is the piezoelectric constants matrix, $\mathbf{E}$ is the electric field vector, $\mathbf{g}$ is the dielectric constants matrix, Ω is the domain occupied by the body and the last term is the external work done. All products are taken as matrix multiplication except where explicit notation is indicated. The external work done by the body force and the surface electrical charge is

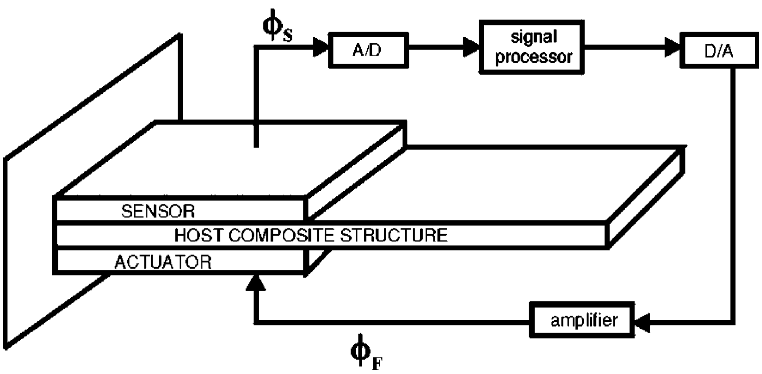

Fig. 1. Schematic of a piezo-elastic composite structure.

$$\sum \mathbf{u}_i \mathbf{f}_i = \int_\Omega \mathbf{u}^\mathrm{T} \mathbf{f} \, \mathrm{d}\Omega - \int_\Gamma \phi Q \, \mathrm{d}\Gamma \tag{2}$$

where $\mathbf{u}(x, y, z)$ is the displacement field vector, $\mathbf{f}$ is the body force vector, $\phi(x, y, z)$ is the electric potential, $Q(x, y)$ is the surface charge and Γ is the boundary of the domain occupied by the body. Given that $\boldsymbol{\varepsilon} = \mathbf{Lu}$ and $\mathbf{E} = -\nabla\phi$, Eq. (1) may be rewritten as

$$W = \frac{1}{2} \int_\Omega \Big(- (\mathbf{Lu})^\mathrm{T} \mathbf{CLu} - 2(\mathbf{Lu})^\mathrm{T} \mathbf{e} \nabla\phi + (\nabla\phi)^\mathrm{T} \mathbf{g} \nabla\phi \Big) \, \mathrm{d}\Omega + \int_\Omega \mathbf{u}^\mathrm{T} \mathbf{f} \, \mathrm{d}\Omega - \int_\Gamma \phi Q \, \mathrm{d}\Gamma \tag{3}$$

where $\mathbf{L}$ is the matrix of differential operators and ∇ is the gradient operator. The stationary condition requires that $\delta W = 0$, where δ is the variational operator.

3. Measurement of potential

One phenomenological characteristic of piezoelectric materials is that application of pressure leads to electric polarisation. By virtue of polarisation charges, an electric field $\mathbf{E}$ exists. This field can be used to identify the shape of the piezo-elastic structure, and may be further processed to provide feedback control. Two approaches in measurement using piezoelectric sensors have been adopted. The first assumes the signal from the sensor to be the electric current, viz. closed circuit mode (Hwang and Park, 1993). The other approach assumes the signal from the sensor to be the potential ϕ, viz. open circuit mode (Wang et al., 1997). The open circuit mode is considered here.

Taking the first variation of the work function in Eq. (3) with respect to the potential, and integrating by parts gradients of the variation of the potential results in

$$\int_\Omega \left(\delta\phi \nabla^\mathrm{T} \mathbf{e}^\mathrm{T} \mathbf{Lu} - \delta\phi \nabla^\mathrm{T} \mathbf{g} \nabla\phi \right) \mathrm{d}\Omega = \int_\Gamma \delta(\phi Q) \, \mathrm{d}\Gamma \tag{4}$$

subject to boundary conditions

$$\int_\Gamma \delta\phi \left(- \mathbf{e}^\mathrm{T} \mathbf{Lu} + \mathbf{g} \nabla\phi \right) \mathrm{d}\Gamma = 0 \tag{5}$$

It follows from Eq. (5) that either the potential ϕ is specified or the electric displacement $\mathbf{D}$, i.e. terms inside the brackets are set to zero on the boundary Γ. Setting the latter to zero requires that the following must be satisfied at the boundary

$$-\mathbf{e}^\mathrm{T} \mathbf{Lu} + \mathbf{g} \nabla\phi = 0 \tag{6}$$

3.1. Current approach

Denote by ϕ_S and ϕ_F the internally generated (sensor) and externally applied (feedback) potential, respectively.

Wang et al. (1997) assumes the charge Q in Eq. (4) to be a constant. This results in the right-hand side of Eq. (4) being given as $\int_\Gamma Q \delta\phi_F \, \mathrm{d}\Gamma$. Subsequently, the displacement-potential relationship is given as

$$-\mathbf{e}^\mathrm{T} \mathbf{Lu} + \mathbf{g} \nabla\phi_S = Q \tag{7}$$

The potential, representative of the piezoelectric sensor signal, is then given as

$$\phi_S = \int_\Gamma \mathbf{g}^{-1} (Q + \mathbf{e}^\mathrm{T} \mathbf{Lu}) \, \mathrm{d}\Gamma \tag{8}$$

3.2. Proposed approach

It is noted that the left-hand side of Eq. (4) considers variations in Ω whereas the right-hand side considers variations in Γ. For uniformity, Gauss' theorem is applied to the right-hand side to associate the variations with Ω, taking into account that the surface charge Q is a function of the potential (Sears et al., 1982). This gives the right-hand side of Eq. (4) as

$$\int_{\Omega} \nabla(\phi_F \delta Q + Q\delta\phi_F)\, \mathrm{d}\Omega \tag{9}$$

Expanding this equation by use of the chain rule, integrating by parts variations of the gradients of the variables, i.e. charge and potential, and grouping like terms together results in

$$\int_{\Gamma} (\phi_F \delta Q|_{\Gamma} + Q\delta\phi_F|_{\Gamma})\, \mathrm{d}\Gamma \tag{10}$$

In Eq. (10), two boundary conditions are obtained as a result of the variational process. These are the potential and charge boundary conditions. Since all variations should vanish at the boundary, either $\phi_F = 0$ or Q is prescribed for the first term, and either $Q = 0$ or ϕ_F is prescribed for the second term. The only condition that can satisfy these boundary conditions simultaneously is $Q = \phi_F = 0$. Enforcing the boundary conditions, Eq. (4) becomes

$$\int_{\Omega} \nabla^{\mathrm{T}}(\mathbf{e}^{\mathrm{T}}\mathbf{L}\mathbf{u} - \mathbf{g}\nabla\phi_S)\, \mathrm{d}\Omega = \int_{\Omega} \nabla^{\mathrm{T}}\mathbf{D}\, \mathrm{d}\Omega = 0 \tag{11}$$

where $\mathbf{D}$ is the electric displacement. This equation describes the divergence of the electric displacement in the domain Ω. To determine the flux of the electric displacement out of the enclosing surface Γ, Gauss' theorem may be used. This gives

$$\int_{\Gamma} \mathbf{D}\, \mathrm{d}\Gamma = 0 \tag{12}$$

As shown in Eq. (11), the electric displacement is divergence free. It follows, from Eq. (12), that the net flux across the surface Γ is zero. That is, the net amount of charge to flow into Ω will be zero. Thus, as much charge flows into Ω as flows out. Subsequently, the displacement-potential relationship may be given as

$$\mathbf{e}^{\mathrm{T}}\mathbf{L}\mathbf{u} - \mathbf{g}\nabla\phi_S = 0 \tag{13}$$

This result shows that Eq. (6) holds on the boundary as well as in the domain occupied by the body. As a result, the potential representative of the piezoelectric sensor signal is

$$\phi_S = \int_{\Gamma} \mathbf{g}^{-1}\mathbf{e}\mathbf{L}\mathbf{u}\, \mathrm{d}\Gamma \tag{14}$$

4. Shape control model

Taking the first variation of the work function, i.e. Eq. (3), with respect to the displacement and integrating by parts the terms with the differential operator $\mathbf{L}$ yields

$$-\int_{\Omega} \delta\mathbf{u}^{\mathrm{T}}(\mathbf{L}^{\mathrm{T}}\mathbf{C}\mathbf{L}\mathbf{u} + \mathbf{L}^{\mathrm{T}}\mathbf{e}\nabla\phi)\, \mathrm{d}\Omega = \int_{\Omega} \delta\mathbf{u}^{\mathrm{T}}\mathbf{f}\, \mathrm{d}\Omega$$

subject to resulting boundary conditions. The coupled piezo-elastic statics equation is given as

$$-\mathbf{L}^{\mathrm{T}}\mathbf{CLu} - \mathbf{L}^{\mathrm{T}}\mathbf{e}\nabla\phi = \mathbf{f} \tag{15}$$

4.1. Current model

The potential in Eq. (15) is de-coupled with the aid of Eq. (8). This gives the uncoupled statics equation in the form of

$$-\mathbf{L}^{\mathrm{T}}\mathbf{CLu} - \mathbf{L}^{\mathrm{T}}\mathbf{eg}^{-1}(Q + \mathbf{eLu}) = \mathbf{f} \tag{16}$$

To effect shape control, the surface charge is assumed to be dependent on the potential (Wang et al., 1997). That is $Q = A_u\phi_S$, where A_u is the proportional gain coefficient. Eq. (8) is then substituted again for the sensor potential ϕ_S, except for the charge Q being set to zero. The current shape control model can thereafter be given as

$$-\mathbf{L}^{\mathrm{T}}\mathbf{CLu} - \mathbf{L}^{\mathrm{T}}\mathbf{eg}^{-1}\mathbf{eLu} - \mathbf{L}^{\mathrm{T}}\mathbf{eg}^{-1}A_u\int_{\Gamma}\mathbf{g}^{-1}\mathbf{eLu}\,\mathrm{d}\Gamma = \mathbf{f} \tag{17}$$

The approach leading to the current shape control model is difficult to comprehend when substitutions are conducted in advance and the resulting expression is substituted into Eq. (15). That is, assume the dependency of the charge on the potential $Q = A_u\phi_S$ and substitute into Eq. (8). Thereafter, substitute Eq. (8) into the equation just found—which is still Eq. (8) expressed differently—and assume $Q = 0$. The result is substituted into Eq. (15) to obtain Eq. (17). This equation may be rewritten as

$$-\mathbf{L}^{\mathrm{T}}\mathbf{CLu} - \mathbf{L}^{\mathrm{T}}\mathbf{e}\nabla\phi - \mathbf{L}^{\mathrm{T}}\mathbf{eg}^{-1}A_u\phi = \mathbf{f} \tag{18}$$

Eq. (18) shows that shape control is depended on the gain and the control potential. At zero gain, i.e. $A_u = 0$, this equation resembles a structure which is not free from piezoelectric control. The middle term on the left-hand side of Eq. (18) represents an inaccessible control state. In order to achieve the full benefit of the control system, all control states must be accessible. Omitting the external force, Table 1 shows configuration states of the current shape control model vs. system requirements as depicted in Fig. 1. The last row of the table indicates that control forces exist at zero amplifier gain contrary to the requirements. Therefore, a model which satisfies the system requirements as depicted in Fig. 1 is proposed.

4.2. Proposed model

In the direct piezoelectric effect, the potential observed across the piezoelectric layer is proportional to the deformation, as shown in Eq. (14). In the absence of passive or active control, the potential will be observed on the piezoelectric layer identified as the sensor as well as the piezoelectric layer identified as the actuator layer. The potential observed on the actuator layer is represented as $\phi_S^{(A)}$. During passive or active control, the potential generated by the actuator layer, $\phi_S^{(A)}$, and the amplified control potential, ϕ_F, coincide. As a result, the effective potential is given as $\phi_{\mathrm{eff}} = \phi_F - \phi_S^{(A)}$. For passive control, the amplified control potential

Table 1
Configuration states of the current model vs. system requirements

Condition	System requirements	Current
$A_u = 0,\ \phi = 0$	$\mathbf{u} = \mathbf{0}$	$\mathbf{u} = \mathbf{0}$
$A_u \neq 0,\ \phi \neq 0$	$\mathbf{u} \neq \mathbf{0}$	$\mathbf{u} \neq \mathbf{0}$
$A_u \neq 0,\ \phi = 0$	$\mathbf{u} = \mathbf{0}$	$\mathbf{u} = \mathbf{0}$
$A_u = 0,\ \phi \neq 0$	$\mathbf{u} = \mathbf{0}$	$\mathbf{u} \neq \mathbf{0}$

is represented in terms of the pre-defined potential. In active control, the amplified control potential is derived from the piezoelectric sensor layer through proportional gain. Hence,

$$\phi_F = A_u\phi_S = \phi_{\text{eff}} + \phi_S^{(A)} \tag{19}$$

Eq. (19) shows that the amplified control potential overcomes the potential generated at the actuator layer before it can effect shape control of the structure. Upon substituting the expression for the control potentials given in Eq. (14) into Eq. (19) and substituting the results into Eq. (15) yields the proposed active shape control model for a piezo-elastic structure as

$$-\mathbf{L}^{\mathrm{T}}\mathbf{CLu} - \mathbf{L}^{\mathrm{T}}\mathbf{e}A_u\mathbf{g}^{-1}\mathbf{eLu} = \mathbf{f} \tag{20}$$

Eq. (20) shows that active shape control is dependant on the gain and the control potential which is derived from the sensor layer. At zero gain, this equation resembles a structure free from any piezoelectric control. This satisfies the system requirements as depicted in Fig. 1.

5. Application to 1-D case

To investigate the proposed model, a symmetrically laminated rectangular beam of length L, width b and thickness h under a transverse bending load q is considered. The beam is constructed of an arbitrary number N of orthotropic layers with fibre orientation θ_k where $k = 1, 2, \ldots, N$. The beam is defined in the Cartesian co-ordinates x, y and z with axes x and y lying on the middle surface of the beam. A first order deformation theory is employed to analyse the problem and the assumed displacement field is

$$\mathbf{u} = \{\, z\psi \quad -w \,\}^{\mathrm{T}} \tag{21}$$

where $\psi(x)$ is the rotation of the transverse normal about the y-axis and $w(x)$ is the deflection of the reference surface in the z-direction. The associated strains are given as

$$\boldsymbol{\varepsilon} = \{\, z\psi_{,x} \quad (\psi - w_{,x}) \,\}^{\mathrm{T}} \tag{22}$$

where the subscript after the comma means differentiation with respect to that variable. Substituting Eq. (22) into Eq. (3) results in

$$W = \sum_{k=1}^{N} \frac{1}{2} \int_{\Omega^{(k)}} \left(-C_{11}^{(k)}(z\psi_{,x})^2 - C_{55}^{(k)}(\psi - w_{,x})^2 - 2z\psi_{,x}e_{31}^{(k)}\phi_{,z}^{(k)} + g_{33}^{(k)}\left(\phi_{,z}^{(k)}\right)^2 \right) \mathrm{d}\Omega + \int_0^L qw\,\mathrm{d}x \tag{23}$$

where, now $\phi = \phi(z)$, $q(x)$ is the distributed load along the length L of the beam and $\mathrm{d}\Omega = \mathrm{d}x\,\mathrm{d}y\,\mathrm{d}z$. Taking the first variation of the work function in Eq. (23) with respect to the potential and integrating by parts terms with the variation of the potential differentiation yields

$$\sum_{k=1}^{N} \int_{\Omega^{(k)}} \delta\phi^{(k)} \left(ze_{31}^{(k)}\psi_{,x} - g_{33}^{(k)}\phi_{,z}^{(k)} \right)_{,z} \mathrm{d}\Omega = 0 \tag{24}$$

subject to boundary conditions

$$\sum_{k=1}^{N} \int_0^L \int_0^b \left(-ze_{31}^{(k)}\psi_{,x} + g_{33}^{(k)}\phi_{,z}^{(k)} \right) \delta\phi^{(k)} \Big|_{h_{k-1}}^{h_k} \mathrm{d}y\,\mathrm{d}x = 0 \tag{25}$$

The boundary conditions in Eq. (25) require that either the electric displacement $D^{(k)} = 0$ or the potential $\phi^{(k)}$ is specified at $z = h_k, h_{k-1}$, where the electric displacement is given by

$$D^{(k)} = -ze_{31}^{(k)}\psi_{,x} + g_{33}^{(k)}\phi_{,z}^{(k)} \tag{26}$$

For non-trivial solutions of Eq. (24) $\delta\phi \neq 0$ is chosen. The electric field is thus given as

$$\phi_{,z}^{(k)} = \frac{1}{g_{33}^{(k)}}(h_k - h_{k-1})e_{31}^{(k)}\psi_{,x} \tag{27}$$

Consequently, the potential becomes

$$\phi^{(k)} = \frac{1}{g_{33}^{(k)}}(h_k - h_{k-1})^2 e_{31}^{(k)}\psi_{,x} \tag{28}$$

The first variation of the work function, i.e. Eq. (23), is carried out with respect to the rotation ψ and integration by parts is applied to terms with the variation of the rotation differentiation. Requiring this variation to vanish for the varied rotation results in

$$\sum_{k=1}^{N}\frac{1}{3}(h_k^3 - h_{k-1}^3)b^{(k)}C_{11}^{(k)}\psi_{,xx} - (h_k - h_{k-1})b^{(k)}C_{55}^{(k)}(\psi - w_{,x}) + b^{(k)}\int_{h_{k-1}}^{h_k}\left(ze_{31}^{(k)}\phi_{,z}^{(k)}\right)_{,x}\mathrm{d}z = 0 \tag{29}$$

The boundary conditions require that either the moment $M = 0$ or the rotation ψ is specified on $x = 0, L$, where the moment is given by

$$M = \sum_{k=1}^{N}\frac{1}{3}b^{(k)}(h_k^3 - h_{k-1}^3)C_{11}^{(k)}\psi_{,x} - b^{(k)}\int_{h_{k-1}}^{h_k} ze_{31}^{(k)}\phi_{,z}^{(k)}\,\mathrm{d}z \tag{30}$$

In feedback applications, the actuator layer is subject to the amplified control potential derived from the potential generated by the piezoelectric sensor layer. This is given as $\phi^{(A)} = G\phi^{(S)}$, where G is the amplifier gain. Thus,

$$b^{(k)}\int_{h_{k-1}}^{h_k}\left(ze_{31}^{(k)}\phi_{,z}^{(k)}\right)_{,x}\mathrm{d}z = b^{(A)}\int_{A_{k-1}}^{A_k}\left(ze_{31}^{(A)}G\phi_{,z}^{(S)}\right)_{,x}\mathrm{d}z \tag{31}$$

where $A, S \in N$ are actuator and sensor layers, respectively. Using Eq. (28) to represent the potential from the piezoelectric sensor layer and substituting into Eq. (29) to decouple the potential yields

$$\sum_{k=1}^{N}\frac{1}{3}(h_k^3 - h_{k-1}^3)b^{(k)}C_{11}^{(k)}\psi_{,xx} - (h_k - h_{k-1})b^{(k)}C_{55}^{(k)}(\psi - w_{,x}) + \frac{1}{2g_{33}^{(S)}}b^{(A)}(h_A^2 - h_{A-1}^2)e_{31}^{(A)}G(h_S - h_{S-1})e_{31}^{(S)}\psi_{,xx} = 0 \tag{32}$$

Using the same to decouple the potential in Eq. (30) gives the moment as

$$M = \sum_{k=1}^{N}\frac{1}{3}(h_k^3 - h_{k-1}^3)b^{(k)}C_{11}^{(k)}\psi_{,x} + \frac{1}{2g_{33}^{(S)}}b^{(A)}(h_A^2 - h_{A-1}^2)e_{31}^{(A)}G(h_S - h_{S-1})e_{31}^{(S)}\psi_{,x} \tag{33}$$

It is noted that the moment in Eq. (33) has two parts, i.e. elastic and piezoelectric. When the gain G is set to zero, the moment will solely be determined by the elastic part. As the gain is varied, the moment will vary proportionally between the elastic and piezoelectric parts.

Following the approach used for the varied rotation, the first variation carried out with respect to the deflection w leads to

$$-\sum_{k=1}^{N}(h_k - h_{k-1})b^{(k)}C_{55}^{(k)}(\psi_{,x} - w_{,xx}) = q \tag{34}$$

The boundary conditions require that either the shear force $V = 0$ or the deflection w is prescribed on $x = 0, L$, where the shear force is given as

$$V = \sum_{k=1}^{N}(h_k - h_{k-1})b^{(k)}C_{55}^{(k)}(\psi - w_{,x}) \tag{35}$$

To investigate the model further, a simply supported beam is considered. Decoupling the rotation and deflection in Eqs. (32) and (34), carrying out the quadratures for ψ and w and using boundary conditions results in the expression for the rotation and the deflection. This is given, respectively, as

$$\psi = \sum_{k=1}^{N} \frac{1}{\left((h_k^3 - h_{k-1}^3)b^{(k)}C_{11}^{(k)}/3 + 1/\left(2g_{33}^{(S)}\right)b^{(A)}(h_A^2 - h_{A-1}^2)e_{31}^{(A)}G(h_S - h_{S-1})e_{31}^{(S)}\right)}\left(\frac{q_0x^3}{6} - \frac{q_0L^2x}{8}\right) \tag{36}$$

$$\begin{aligned} w = {} & \sum_{k=1}^{N} \frac{q_0}{2(h_k - h_{k-1})b^{(k)}C_{55}^{(k)}}\left(\frac{L^2}{4} - x^2\right) \\ & + \frac{q_0}{\left((h_k^3 - h_{k-1}^3)b^{(k)}C_{11}^{(k)}/3 + 1/\left(2g_{33}^{(S)}\right)b^{(A)}(h_A^2 - h_{A-1}^2)e_{31}^{(A)}G(h_S - h_{S-1})e_{31}^{(S)}\right)}\left(\frac{x^4}{24} - \frac{L^2x^2}{16} + \frac{5L^4}{384}\right) \end{aligned} \tag{37}$$

6. Numerical results

A simply supported beam subjected to a uniform load of unit magnitude is considered. Attached to the beam are collocated piezoelectric elements spanning its entire length. Material properties used to investigate

Table 2
Material properties

Property	PZT-5A	Graphite/epoxy
C_{11} (GPa)	66.0	23.16
C_{55} (GPa)	21.0	7.85
e_{31} (C/m^2)	−12.54	0.0
g_{33} (pF/m)	15.937	0.0
Width (mm)	31.8	32.5
Thickness (mm)	0.05	1.0

Table 3
Maximum responses at zero gain

Maximum response	x/L	Passive	Current	Proposed
Deflection (m)	0.5	0.1080	0.1042	0.1080
Rotation (rad)	0.0	0.3454	0.3335	0.3454
Shear force (N)	0.0	−0.500	−0.500	−0.500
Moment (N/m)	0.5	−0.125	−0.125	−0.125

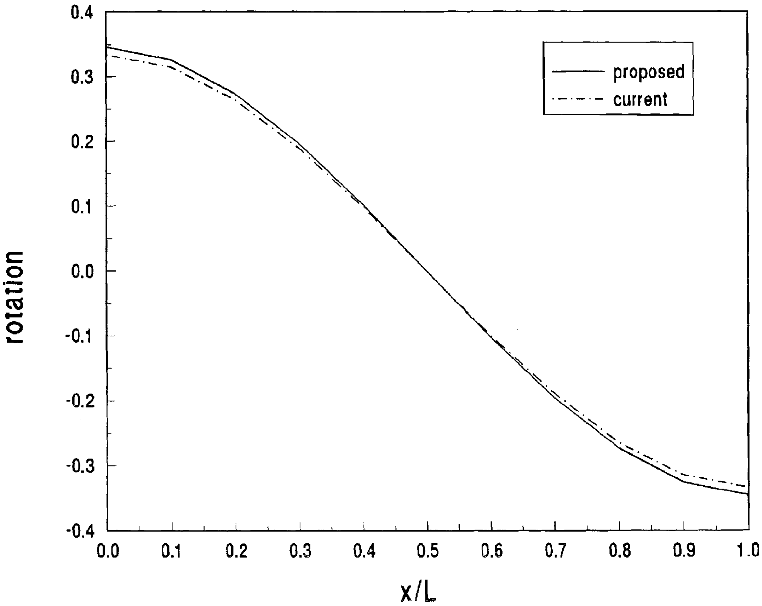

Fig. 2. Rotation of beam fibres at zero gain.

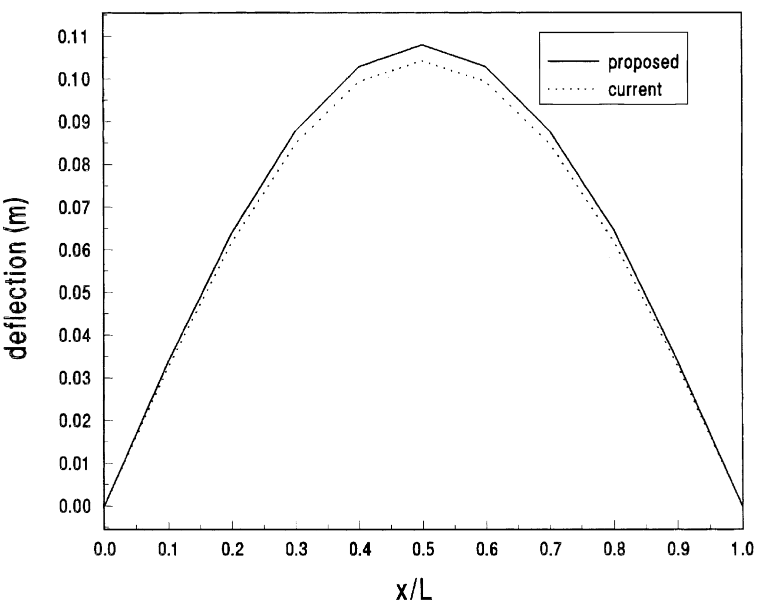

Fig. 3. Deflection of the mid-surface at zero gain.

the current and proposed shape control models are shown in Table 2. Table 3 shows the extreme responses for the current and proposed model at zero gain versus the passive structure.

Table 4
Percentage moment distribution at the centre of the beam

Model	Moment	Gain	Percentage of elastic	Percentage of piezo
Current	0.125	0	96.5365	3.4635
	0.125	1	0.8810	99.1190
	0.125	10	0.0888	99.9112
	0.125	100	0.0089	99.9911
Proposed	0.125	0	100	0
	0.125	1	99.6597	0.3403
	0.125	10	96.6984	3.3016
	0.125	100	74.5471	25.4529

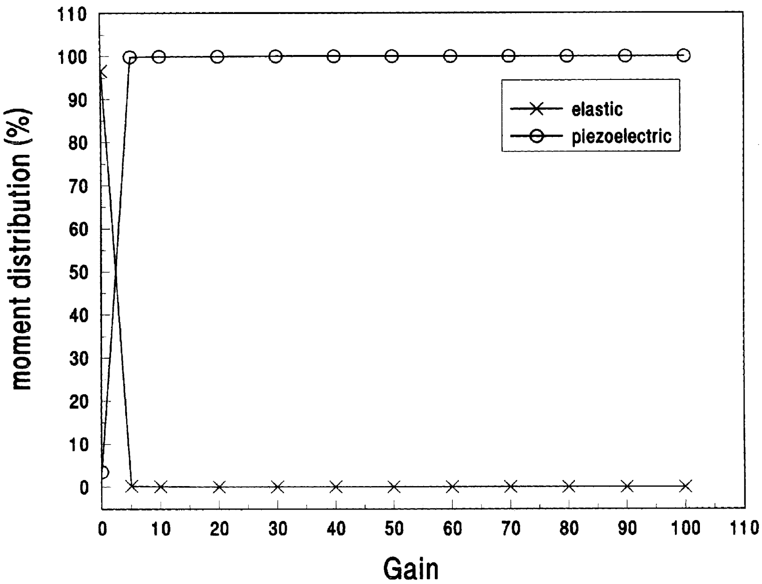

Fig. 4. Percentage moment distribution for current model.

In Table 3, it can be seen that for deflection and rotation, the proposed model resembles the passive structure at zero gain whereas the current model does not resemble the passive structure, though it is not far out. The fictitious stiffness introduced by the inaccessible control state inherent in the current model brings about this error. However, the current and proposed models are moment preserving. This indicates that the net elastic and piezoelectric effects preserve the moment due to the external force. Figs. 2 and 3 show the rotation of the transverse normal and the deflection of the reference surface, respectively, across the length of the beam at zero gain.

Table 4 shows the percentage moment distribution at selected gains. The current model depicts a cross-over redistribution of the elastic and piezoelectric effects when it is varied from zero. Thereafter, the distribution changes slightly (see Fig. 4). For the same range, the proposed model gives a linear redistribution between the elastic and piezoelectric effect (see Fig. 5). Fig. 6 shows the maximum deflection at various gain using the current model. In this figure, there is an abrupt change of the deflection just after zero gain. This

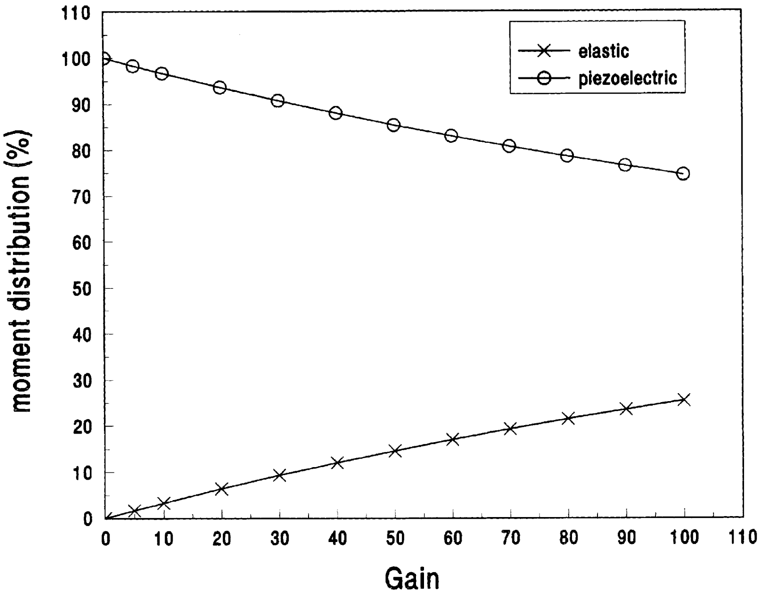

Fig. 5. Percentage moment distribution for proposed model.

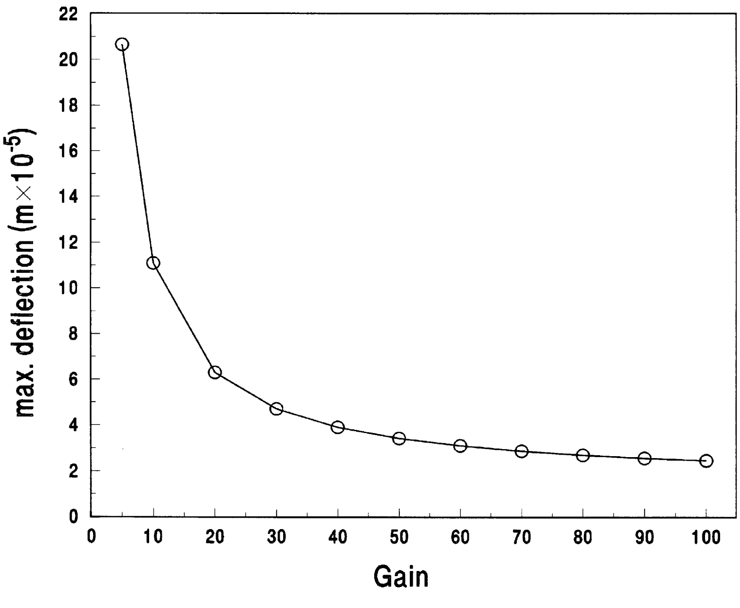

Fig. 6. Maximum deflection vs. gain for current model.

accounts for the cross-over moment redistribution seen before. Thus, the stiffness due to the piezoelectric effect, as depicted by the current model, is greater than that of the elastic property by a high order. Fig. 7 shows the maximum deflection at various gains using the proposed model. In this figure, the deflection decreases linearly with an increase in gain.

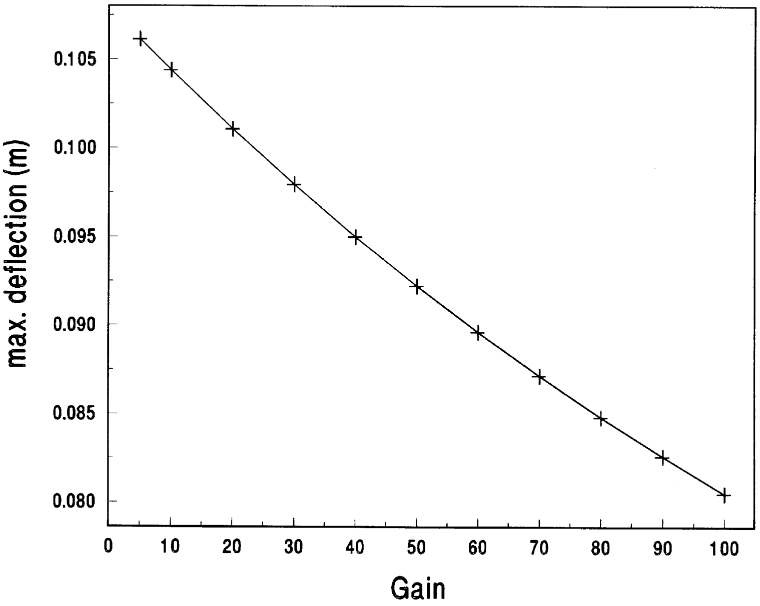

Fig. 7. Maximum deflection vs. gain for proposed model.

7. Conclusion

The study proposes a control model of the open circuit mode which resembles the passive structure at zero gain. This model results from showing that the electric displacement is divergence free, thus indicating the non-controlling effect of the applied electric charge. On the contrary, the existing control model is formulated assuming the charge to be a function of the potential.

A simply supported composite beam attached with collocated piezoelectric elements for measuring and actuating was considered. At zero gain, results show that the current control model introduces a fictitious stiffness due to the inherent inaccessible state. Thereafter, a cross-over in piezoelectric and elastic moment percentage redistribution is observed when the gain is increased. Also, the displacement changes abruptly. A further increase in gain results in a relatively minute change in the moment percentage redistribution and the displacement.

For the proposed model, results show that it predicts realistic behaviour for piezo-elastic structures. That is, at zero gain the proposed model resembles a structure, which is free from piezoelectric control. An increase in gain results in a proportional change in the deflection as well as a linear percentage moment redistribution between the piezoelectric and elastic stiffness.

It follows that a physical piezo-elastic structure that is built based on the analysis of the current control model will exhibit a strength capability different to one predicted by the analysis. However, a further investigation needs to be conducted to compare results of the proposed control model with experimental ones.

Acknowledgement

The authors acknowledge the financial support of the National Research Foundation of South Africa (GUN 2045467).

References

Cady, W.G., 1946. Piezoelectricity. McGraw–Hill.

Chandrashekhara, K., Donthireddy, P., 1997. Vibration suppression of composite beams with piezoelectric devices using a higher order theory. European Journal of Mechanics, A/Solids 16 (4), 709–721.

Detwiler, D.T., Shen, M.-H.H., Venkayya, V.B., 1995. Finite element analysis of laminated composite structures containing distributed piezoelectric actuators and sensors. Finite Element in Analysis and Design 20, 87–100.

Hwang, W.S., Park, H.C., 1993. Finite element modelling of piezoelectric sensors and actuators. AIAA Journal 31 (5), 930–937.

Kekana, M., 2001. Stability of a shape control model for piezoelectric structures. In: Proceedings of the Eighth International Conference on Composites Engineering, Spain.

Kekana, M., 2002. A static shape control model for piezo-elastic composite structures. Composite Structures 59 (1), 129–135.

Kekana, M., Walker, M., 2001. Stability of a finite element model used to simulate the vibration of piezoelectric structures. In: Proceedings of the Seventeenth International Conference on CAD/CAM, Robotics and Factories of the Future, Durban.

Miller, S.E., Abramovich, H., Oshman, Y., 1995. Active distributed vibration control of anisotropic piezoelectric laminated plates. Journal of Sound and Vibration 183 (5), 797–817.

Sears, F.W., Zemansky, M.W., Young, H.D., 1982. University Physics, sixth ed Addison-Wesley Publishing Company.

Tzou, H.S., Tseng, C.I., 1990. Distributed sensor/actuator design for dynamic measurement/control of distributed parameter systems: a piezoelectric finite element approach. Journal of Sound and Vibration 138 (1), 17–34.

Tzou, H.S., Tseng, C.I., 1991. Distributed vibration control and identification of coupled elastic/piezoelectric systems: finite element formulation and applications. Mechanical Systems and Signal Processing 5 (3), 215–231.

Wang, Z., Chen, S., Han, W., 1997. The static shape control for intelligent structures. Finite Elements in Analysis and Design 26, 303–314.

Yin, L., Shen, Y., 1997. Strain sensing of composite plates subjected to low velocity impact with distributed piezoelectric sensors: a mixed finite element approach. Journal of Sound and Vibration 199 (1), 17–31.